

Network topology of the Euro Area interbank market

Ilias Aarab

Thomas Gottron

European Central Bank,* Sonnemannstraße 20, Frankfurt am Main, Germany

Ilias.Aarab@ecb.europa.eu

Thomas.Gottron@ecb.europa.eu

Date: 20/10/2022

Abstract

The rapidly increasing availability of large amounts of granular financial data, paired with the advances of big data related technologies induces the need of suitable analytics that can represent and extract meaningful information from such data. In this paper we propose a multi-layer network approach to distill the Euro Area (EA) banking system in different distinct layers. Each layer of the network represents a specific type of financial relationship between banks, based on various sources of EA granular data collections. The resulting multi-layer network allows one to describe, analyze and compare the topology and structure of EA banks from different perspectives, eventually yielding a more complete picture of the financial market. This granular information representation has the potential to enable researchers and practitioners to better apprehend financial system dynamics as well as to support financial policies to manage and monitor financial risk from a more holistic point of view.

Keywords: granular data collections, network topology, interbank system, multi-layer networks

Introduction

The approach of modelling the banking sector as a network of interconnected entities has received increasing attention in recent years [18]. The increased attention is driven by the demand to better understand the complexity of interrelations between banks after the 2008 financial crisis, where mechanisms of an interwoven financial system were difficult to understand and predict. Consequently, more and more granular data¹ about the financial and banking system is made available to supervisors to fuel analytical models capturing interdependencies in the market.

*The views expressed in this paper are those of the authors and do not necessarily reflect those of the European Central Bank.

¹In the given context, granular data refers to detailed, specific, and finely segmented information about individual components or entities within the financial and banking system. This data provides a detailed view of individual banks, financial institutions, or other entities, including their transactions, interactions, and various aspects of their operations.

Related literature can be divided into two categories: (1) motivating work, arguing for the advantages of modelling financial markets as networks, and (2) empiric work, using different types of data to describe certain aspects of the network structures in the banking sector.

As argued by [3], the use of network theory can help in understanding financial systems, the interactions among agents and certain economic phenomena. According to [5], the complex network of exposures among banks can be considered as one of the key features for determining systemic risk while [14] review network-based approaches as analytical basis for systemic risk indicators. Recent work focuses in particular on multi-layer networks [6]. Multi-layer networks cater for the different types of interrelation among banks and model them separately in distinct layers of the network, where each layer may exhibit a different topology [7].

Empirical work analysing interbank networks is mainly driven by the availability of data. Relevant papers range from descriptive approaches to investigating the network topology to applying novel analytical frameworks to the data. [11] analysed Austrian banks based on general network theory methods and showed that the degree distribution in the network follows a powerlaw distribution, that the network has a low clustering coefficient and a short average path length. Key insights regarding the topology of an emerging network are that a core-periphery structure describes the network better than other generative models [1]. Empirical investigations of multi-layer networks capture different types of connections between banks. [6] distinguish between maturity and the secured or unsecured nature of the contracts among banks on the Italian market and showed how the resulting layers are of quite different topology. Moreover, a flattened and aggregated representation of all layers is not suitable to capture the full complexity of the network. [22] develop their model for assessing systemic risk on a multi-layer network of short-term and long-term loans and the common exposures to financial assets due to overlapping portfolios. [2] use data on exposures between large European banks, broken down by maturity and instrument type to characterise the main features of a multi-layer network.

In this paper, we highlight the utility of granular data collections for constructing and analyzing multi-layer networks. Granular data offers flexibility in filtering, aggregation, and focus, enabling the construction of diverse network models from the same source data. Additionally, specific instances of networks can serve multiple analytical purposes and answer various questions. We demonstrate the construction of a multi-layer network covering the broad scope of the EA financial market using data from different granular collections, detailing the preprocessing, integration, and aggregation methods applied. We present analytical tasks, implemented approaches, and insights gained from the analysis, aligning real-world data results with theoretical expectations.

Data

Diverse granular datasets serve as the fundamental basis for constructing our multi-layer networks. In the subsequent sections, we explain their distinct characteristics and provide a rationale for their selection in

our analysis:

Register of Institutions and Affiliates Data (RIAD): RIAD is the shared master dataset serving several European System of Central Banks (ESCB) and Single Supervisory Mechanism (SSM) business processes and statistical data collections. The RIAD data model includes more than 100 properties for legal entities, including a wide range of entity identifiers and relationships (e.g. foreign branches, subsidiaries). In our application, RIAD served to identify entities across different datasets and as source for constructing banking groups.

List of significant banking groups (ROSSI list): All of the granular datasets considered in this work comprise various information on the largest banking groups in the EA and participating member states which are directly supervised by the SSM. Therefore, the ROSSI list is used to determine the sample of banking groups to be included in our multi-layer network. As of 1st of June 2021, this list of significant institutions comprised a total of 114 banking groups. From ROSSI, we extract the RIAD codes of significant institutions, considering the prudential consolidation regime. This regime widens the group structure view as it also considers cases where the consolidating entity might be different than a bank (e.g. financial holding) and improves consistency in the aggregation of granular datasets.

CSDB and SHSG data: The Centralised Securities Database (CSDB) is a reference database for all securities relevant for statistical purposes of the ESCB. It comprises information on debt securities, equity instruments and investment fund shares which are stored on a security-by-security basis. Each instrument is identifiable by its International Securities Identification Number. While CSDB covers the issuance of securities by banking groups, the Securities Holdings Statistics Database by Group (SHSG) dataset contains the holdings of securities by banks. Thus, using both databases we gain insights into the securities being issued by banking groups as well as the securities they are currently holding.

AnaCredit data: The AnaCredit dataset contains loan-by-loan information on loans extended to corporations collected from EA banks. This data is reported at monthly frequency starting from September 2018. Among others, information on the outstanding amount, maturity, interest rate, collateral/guarantee, and on involved counterparties is collected for each of the individual loans.

SFT – Securities Financing Transactions data: The Securities Financing Transactions Data Store (SFTDS) collects and processes data reported under the Securities Financing Transactions Regulation (EU) 2015/2365². SFTs and the scope of the SFTR include³: (a) repurchase/ reverse repurchase transactions, (b) buy-sell back or sell-buy back transactions, (c) securities or commodities lending and securities or commodities borrowing and (d) margin lending transactions.

FINREP/COREP: FINREP (Financial Reporting Standards) and COREP (Common Reporting Stan-

²Regulation (EU) No. 2015/2365 on transparency of securities financing transactions and of reuse and amending Regulation (EU) No. 648/2012 Securities Financing Transactions Regulation – SFTR).

³Article 3 (11) SFTR

dards) are the two reporting frameworks developed as part of the implementation of Basel III in Europe⁴ which gives the European Banking Authority the legal basis to request both capital and financial information from EA banks. COREP specifies the framework related to capital information, while FINREP specifies the financial information. Banks subject to International Financial Reporting Standards (IFRS) already use the FINREP templates to submit financial information in a harmonised format at consolidated level. This requirement has also been extended to SSM banks reporting at sub-consolidated or solo level under IFRS and national Generally Accepted Accounting Principles (GAAPs)⁵. FINREP templates are subject to a quarterly mandatory reporting. COREP is used to collect Pillar 1 data and information on liquidity, leverage and large exposures from banks in a harmonised format.

Network modelling

Identification and modelling of banking groups

The first step in modelling a multi-layer network is to define the nodes n_i of the network. As our main focus is to model the exposures between banking groups across different markets, we model banking groups as nodes. The construction of banking groups is initiated from the head of a banking group. The list of group heads of significant⁶ banks in the EA was retrieved from ROSSI. Upon identifying the group head, we discern all entities affiliated with the respective group. A subsidiary of a group is identified as an entity on which the group head exercises direct or indirect control, based on equity share⁷. To obtain a complete group structure, including subsidiaries that are not credit or financial institutions, we leverage and integrate different group information available in ROSSI, COREP and RIAD.

Granular data integration

After the identification of banking groups and their subsidiaries, we integrate the different granular datasets as basis for forming the interactions between groups. Consistent identification of group entities is realised using entity identifiers available in RIAD. During the integration process we also harmonise and align different structures and semantics of the various datasets (e.g., stock-based vs. transactional data). Having information on the banking group structure allows us to aggregate information on subsidiaries to the

⁴EBA's Implementing Technical Standards (ITS) amending the European Commission's Implementing Regulation (EU) No 680/2014 on supervisory reporting of institutions under Regulation (EU) No 575/2013.

⁵Regulation (EU) 2015/534 of the ECB of 17 March 2015

⁶The definition of Significant Institutions can be found in Regulation (EU) No 468/2014 of the European Central Bank of 16 April 2014.

⁷In addition, supervised entities according to Guideline (EU) 2020/497 of the ECB are also included in the group, if not already included following the control relationship criteria.

group head level and identify interrelations across all granular datasets⁸.

Construction of a multi-layer network

We follow [7] and define a multi-layer network as a network where each node appears in a set of different layers ℓ , and each layer describes all the edges of a given type. In our case, the edges e_{ij}^ℓ from node n_i to node n_j are directed and their weight indicates the aggregated exposure of banking group n_i towards n_j within layer ℓ ⁹. The edge values differ across the layers ℓ based on the type of exposure they represent:

Long-term credit layer: This layer contains loan exposures between banking groups having an initial maturity of at least three months, in line with [22]. Exposures are aggregated over different types of loan instruments (e.g., deposits, credit lines, convenience credit, etc.), with the bulk (more than 90%) of exposures coming from deposits, credit lines other than revolving credit and unspecified loans. Edge weights e_{ij}^{lc} indicate the outstanding nominal values.

Short-term credit layer: This layer contains loan exposures with an initial maturity shorter than three months. Exposures are processed in the same way as for the long-term credit layer, with the additional constraint of ensuring strictly positive maturities of the loans. We observe that a large part of instruments (more than 45%) are reverse repurchase agreements confirming the short-term nature of the layer. Edge weights e_{ij}^{sc} indicate the outstanding nominal values.

Cross-securities layer: This layer contains equity and debt holdings between banking groups. An edge from node n_i to node n_j represents the market value of the securities issued by n_j and held by n_i . We do not distinguish between equity and debt-based securities and aggregate them together into the same edge. The edge weight e_{ij}^{cs} represents the market value of investments made by n_i into n_j 's issued securities.

Short-term funding layer: The short-term funding layer contains repurchasing agreements and buy-sellback information obtained from the SFT dataset. Within this layer an edge from node n_i to n_j represents the (aggregated) open funding transactions between banking group n_i and n_j . The edge e_{ij}^{sf} is directed from the collateral taker to the collateral giver. To integrate the resulting data with the other granular datasets, we extract those transactions that are indicated as active at the end of a month as they represent a snapshot of the end-of-month exposures of banking groups.

Overlapping portfolio layer: The overlapping portfolio layer models the investments made by banking groups in securities that are issued by entities that are not part of the interbank market. We are particularly interested in the way that this layer can induce potential fire sales effects. To model this behaviour in a straightforward manner, we create an undirected graph where an edge e_{ij}^{op} between banking group n_i and banking group n_j represents the market value of the overlapping part of their portfolios. In this manner, the

⁸To efficiently process the large amount of data we make use of a Hadoop based data lake to store the data and utilize Spark for distributed processing.

⁹Note that intra-group exposures of banking groups are removed to avoid self-loops within the network.

effect of a sell-off of n_i 's securities, can be traced back by following the edges that are (directly or indirectly) connected with n_i . To contain the universe of possible securities, we aggregate them on the issuer level. This approach offers the added advantage of implicitly accounting for the positive correlations among securities issued by the same issuer.

Flattened network layer: The flattened network layer is an artificially constructed layer, in the sense that it does not represent a specific real-world market. Instead, the layer is defined as the aggregation of all of the layers of the multi-layer network. More specific, we follow [7] and create a weighted aggregated overlapping adjacency matrix to form the flattened network layer.

Enrichment of the nodes

After constructing the multi-layer network, we further enrich the nodes of the network. The goal is to describe the nodes through their most relevant balance sheet items like the Tier 1 Capital and Total Assets. These balance sheet values are retrieved from FINREP¹⁰ and COREP¹¹ templates, where the values are available at a consolidated level allowing for a mapping to the banking groups via RIAD identifiers.¹²

Network topology

To dig deeper into the topology of the constructed multi-layer network, we leverage both graph statistics, which describe the overall network structure, and centrality measures aimed at characterizing individual nodes within the system. As seen in related work [6], this is of particular interest, as the different semantics of the layers in a multi-layer network entail different topologies and structures. The use of graph statistics jointly with centrality measures is necessary, as congruence of topology between two or more layers (graph statistics) does not necessarily imply point-wise similarity between the nodes in the layers (centrality measures) [15].

Graph statistics

Table 1 presents an overview of the global graph metrics across the different layers. The multi-layer network encompasses 114 banking groups interacting across its various layers. Notably, the overlapping portfolio layer exhibits significant interconnectedness, evidenced by 3,614 edges. In contrast, both the short-term and long-term interbank credit layers, along with the short-term funding layer, display sparser

¹⁰Total assets are available in FINREP template: F 01.01 - Balance Sheet Statement.

¹¹Tier 1 Capital is available in the COREP template: C47.00 – Leverage ratio calculation. The amount of Tier 1 capital is calculated according to article 25 of the CRR, without taking into account the derogation laid down in Chapters 1 and 2 of Title I of Part Ten of the CRR.

¹²Note that the analysis we conduct focuses on a static snapshot of the multi-layer network. The considered snapshot is the end-of-month observation of the network as of June 2021. This is a date in which all datasets, considering their respective frequencies, are available.

Table 1: Graph statistics across network layers

	ST credit	LT credit	Cross-sec.	ST funding	Overlap	Overlap (dir.)	Flattened
Nodes (N)	114	114	114	114	114	114	114
Edges (E)	525	901	2,456	900	3,614	3,614	2,969
Connected components	26	14	11	42	13	13	4
Largest component: share of nodes	0.78	0.88	0.91	0.64	0.89	0.89	0.97
Largest component: share of edges	0.79	0.76	0.77	0.65	1.00	1.00	0.71
Diameter (largest component)	5	4	5	4	2	2	4
Avg. clustering coefficient	0.29	0.38	0.51	0.41	0.79	0.39	0.62
Reciprocity	0.42	0.48	0.47	0.71	0.00	0.00	0.58
Density	0.04	0.07	0.19	0.07	0.56	0.28	0.23
Global efficiency	0.30	0.40	0.55	0.24	0.68	0.68	0.63
Herfindahl index	0.05	0.04	0.02	0.04	0.07	0.07	0.04

Notes: ST = short-term; LT = long-term; Cross-sec. = cross-securities; dir. = directed (symmetrized) version of the overlapping-portfolio layer.

connectivity, with densities ranging from 4% to 7%. The cross-securities layer falls between these extremes, featuring 2,456 interlinkages among the agents.¹³

Although no layer is fully connected, a significant majority of nodes belong to the largest connected component¹⁴ within each layer. Specifically, in the cross-securities and credit layers, approximately 80-90% of nodes are part of the largest subcomponent. In the short-term funding layer, this proportion reduces to 64% of agents forming the largest component. Notably, in the overlapping portfolio layer, 90% of nodes constitute the largest component; all realized edges are within this component, suggesting that the remaining agents exist as isolated islands.

The diameters of the various layers support these observations. The largest shortest distance between any two agents is approximately four to five edges for the credit, cross-securities, and funding layers, while it is only two edges for the overlapping portfolio layer. This suggests that fire sales by agents can propagate much more rapidly through the network in comparison to default cascading effects observed in the other layers.

Turning to the clustering of nodes, Table 1 displays the average clustering coefficients across the markets. The clustering coefficient ranges from 29% (short-term credit layer) to 51% (cross-securities layer).¹⁵ These

¹³To have a meaningful comparison between the layers, we transform the undirected overlapping portfolio layer into a directed symmetric graph.

¹⁴A connected component is a set of nodes which are directly or indirectly connected to each other. From the perspective of a specific node, it is not possible to reach any node outside the component it belongs to.

¹⁵It is worth mentioning that the clustering coefficient of the overlapping portfolio layer is substantially higher due to its undirected nature. Assuming a directed graph, the clustering coefficient aligns more closely with other layers at 39%.

values are consistent with empirical observations in other interbank markets ([25]; [6]). In conjunction with the low diameters, all layers demonstrate potential small-world properties as defined by [30]. To explore this further, we follow the approach of [13] and analyze the relationship between degree distributions and clustering coefficients across the layers. Figure 1 illustrates the results. Despite some noise, an overall negative relationship between these metrics is apparent. This suggests that highly connected agents tend to interact with counterparties who have limited interactions with each other, typically smaller entities. This observation indicates the presence of smaller-sized hubs connecting diverse market participants. In contrast, agents with lower degrees are interconnected with counterparties who are densely connected with each other, encompassing varying entity sizes, including the largest agents. This configuration hints at the existence of stable and robust relationships among certain agents. Notably, only in the overlapping portfolio layer can we confirm that the clustering coefficient is bounded away from zero. Thus, unlike other layers and in conjunction with the graph statistics, the overlapping portfolio layer stands out as a potential small-world graph.

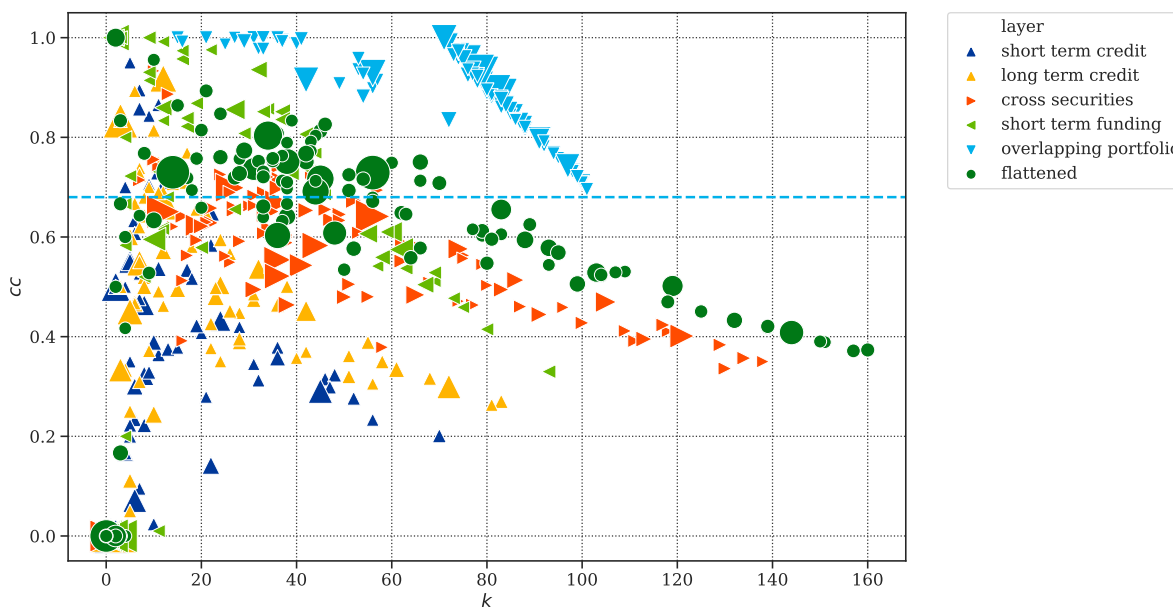


Figure 1: Relationship between the degree (k) and clustering coefficient (cc) of banking groups within the multi-layer network. Each layer is color-coded, and the size of the markers is proportional to the total assets of the banking groups. The figure has been created using [17].

Scale-free properties

Theoretical literature on interbank networks typically assume so-called scale-free networks when simulating plausible interbank networks (e.g.; [16], [23] and [24]) These types of networks commonly rely on specific statistical properties of the tails of the degree distributions underlying the networks. Technically,

scale-free networks are loosely described by a probability density function which can be modelled by a power law functional relation, at least asymptotically. In this section, we examine the multi-layer network to determine whether these assumptions in literature are in line with empirical findings and how these findings might change across the different layers in the network. The premise about the potential of scale-free networks to capture the underlying network topology of interbank markets holds great importance for economic policy [22]. Contagion models often rely on scale-free topologies to simulate an interbank network (e.g. [24]), which has direct consequences on various policy implications [8].

Our analysis focuses on the distribution of the weighted in-degree of the entities in the multi-layer network. The weighted in-degree of an entity $K_{weighted}^{in}(i)$, represents the total of exposures connected to that entity n_i . E.g., for the long-term credit market $K_{weighted}^{in}(i)$ is equal to the total amount that n_i has borrowed from various creditors belonging to banking groups where n_i is not part of. A similar analysis can be set-up for the weighted out-degree $K_{weighted}^{out}(i)$.

We consider the set of statistical distributions depicted in Table 2 as the candidates to fit $K_{weighted}^{in}(i)$.¹⁶ The power law distribution is of main interest as this gives most evidence of the existence of scale-free networks and is usually embedded in the generating process when simulating such networks [12]. We also consider the truncated power law which behaves similar to the power law but converges towards an exponential distribution as we move deeper into the tails. Next, we consider the lognormal distribution due to its flexibility of capturing heavy tails [1]. Lastly, we consider the exponential distribution which is, per definition, the minimum alternative candidate for evaluating the existence of heavy-tails, as heavy-tailed distributions are usually defined as not exponentially bounded [20].

Table 2: Statistical distributions to approximate empirical data

Name	functional form $f(\mathbf{x})$	normalization constant C
Power law	$x^{-\alpha}$	$\frac{1}{\zeta(\alpha, x_{\min})}$
Truncated power law	$x^{-\alpha}e^{-\lambda x}$	$\frac{\lambda^{1-\alpha}}{\Gamma(1-\alpha, \lambda x_{\min})}$
Lognormal	$\frac{1}{x} \exp\left(-\frac{(\ln x - \mu)^2}{2\sigma^2}\right)$	$\left[\sigma\sqrt{2\pi} \cdot \frac{1}{2} \operatorname{erfc}\left(\frac{\ln x_{\min} - \mu}{\sqrt{2}\sigma}\right)\right]^{-1}$
Exponential	$e^{-\lambda x}$	$(1 - e^{-\lambda})e^{\lambda x_{\min}}$

Figure 2 plots the empirical probability density functions (PDFs, blue markers). For each of the different layers in the multi-layer network we fit the candidate distributions using the method of maximum likelihood. In other words, we utilize the respective Maximum Likelihood Estimators (MLEs) of the candidates to find

¹⁶The third column of Table 2 shows the normalization constant C such that $\sum_{x=x_{\min}}^{\infty} Cf(x) = 1$.

the best fitting parameter(s) to describe the empirical observations. The left column of Figure 2 overlays the fitted candidate distributions when using all of the empirical data. The right column of Figure 2 represents the same information as the first column, but here we use the optimization scheme of [12] to fit a (truncated) power law to only the (estimated) tail of the empirical distributions.

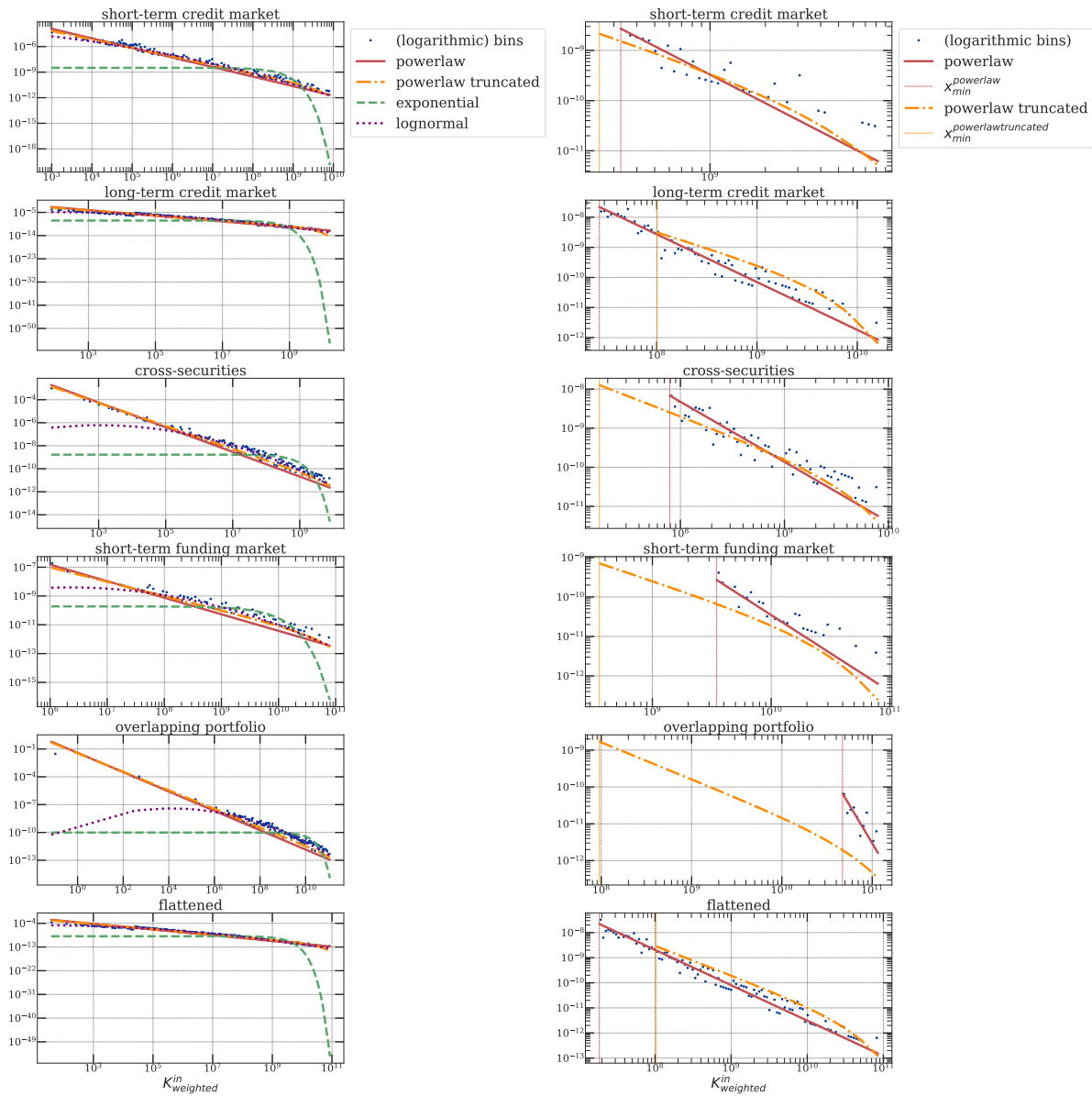


Figure 2: The figure shows the empirical probability density functions (PDFs) over the entire data-range (left column) as well as their tail-only estimation (second column). Empirical PDFs are estimated using logarithmic binning in combination with the normalizing scheme of [21]. Empirical PDFs are depicted by the centre of these logarithmic bins as blue markers presented on logarithmic spaced axes (log-log axes). Fitted candidate distributions are presented as colour coded lines. Candidate distributions are fitted by following the methodology depicted in [12], and utilizing the Python libraries offered by [28] and [4]. The figure has been created using [17].

In all layers, we observe weighted in-degree exposures spanning several orders of magnitude, indicating

a heavy-tailed distribution. In the short-term credit layer, the empirical probability density function (PDF) appears relatively linear, with most candidate distributions fitting the data well except for the exponential distribution. Focusing on the right column of Figure 2, both the truncated and the traditional power law models estimate the start of the tail distribution, denoted as x_{min} , at approximately 30×10^7 EUR, roughly the 80th percentile. The long-term credit layer and the flattened layer exhibit similar characteristics. The exponential distribution misfits the data from the short-term credit, cross-securities, short-term funding, and overlapping portfolio layers, whereas the truncated and the traditional power law models better capture the entire data range. Notably, tail estimation for the short-term funding layer significantly differs between the truncated and traditional power law, with the power law estimating a narrower tail. Tail estimations for the overlapping portfolio layer appear problematic, with estimated lower bounds of the tails nearing the upper edge of the distribution. This suggests that no discernible difference exists between the bulk data and its tail. For such estimations the identified tail does not hold a sufficient amount of data points to perform a meaningful fit.

To quantitatively determine which candidate best fits the empirical data, we leverage the following pairwise likelihood ratio test \mathcal{R} :

$$\mathcal{R}(p_1, p_2) = \sum_{i=1}^N [\ln p_1(x_i) - \ln p_2(x_i)].$$

With $p_1(x)$ and $p_2(x)$ the PDFs of the theoretical distributions and N the total number of empirical observations. A positive value indicates that $p_1(x)$ fits the data better than $p_2(x)$. To determine the best fitting distribution out of all candidates, we employ a similar methodology as [27], where we compute the following scores:

$$g(p_k) = \sum_{l \neq k} [\mathcal{R}(p_k, p_l) \text{ if p-value} \leq 0.05]$$

With k and l one of the candidate distributions. The candidate with the highest score is deemed the most suitable theoretical distribution to explain the observed data.

Semi-parametric bootstrapped goodness-of-fit

Likelihood-ratio tests only indicate which candidate distribution provides the *relatively* better fit to the empirical data; they do not imply that the best-performing candidate is an *adequate* description of the data-generating process. In fact, for any empirical sample one can typically fit some theoretical distribution. To assess absolute fit, [12] propose a semi-parametric bootstrap procedure for goodness-of-fit testing of heavy-tailed distributions, which also applies when the tail is fitted above an estimated cut-off value \hat{x}_{min} .

The bootstrap procedure is summarized in Figure 3, and the results for the full empirical range (bulk + tail) are reported in Figure 4. Guided by the likelihood-ratio outcomes, we apply this scheme to test whether a truncated power law provides an adequate fit to the empirically observed degree distributions in each layer.

Table 3: Best-fitting distributions (bulk + tail)

Layer	Best fit	Score	Runner-up	LR test (\mathcal{R})
Short-term credit	Truncated power law	27.47	Lognormal	-0.53**
Long-term credit	Truncated power law	41.43	Lognormal	-17.47***
Cross-securities	Truncated power law	57.62	Lognormal	-7.79***
Repo market	Truncated power law	18.93	Lognormal	-2.48*
Overlapping portfolio	Truncated power law	129.80	Lognormal	-11.75***
Flattened network	Truncated power law	48.81	Lognormal	-21.73***

Notes: The last column reports the likelihood-ratio statistic \mathcal{R} comparing the best fit against the runner-up. ***, **, and * denote significance at the 1%, 5%, and 10% levels, respectively, following [29].

The null hypothesis, H_0 , is that the data are generated by a truncated power law. More precisely, H_0 states that the (positive) Kolmogorov–Smirnov distance between the empirical distribution and the fitted truncated power law can be attributed to statistical fluctuations under the truncated power-law data-generating process. We simulate B bootstrap samples from the fitted model, re-estimate the parameters on each synthetic sample, and recompute the Kolmogorov–Smirnov distance. If the empirical distance is large relative to the bootstrap distribution (i.e., many bootstrap distances are smaller than the empirical one), then H_0 is unlikely and should be rejected. We use a conservative confidence level of 10%¹⁷ to decide on rejection.

As shown in Figure 4, for all layers we fail to reject H_0 , and thus find evidence that the (weighted) degree distributions are consistent with a truncated power law. The empirical Kolmogorov–Smirnov distances are sufficiently small relative to their bootstrap counterparts to be plausibly explained by sampling variability, suggesting that these markets are governed by a truncated power-law data-generating mechanism. The layers are also broadly consistent in terms of parameter estimates, with $\alpha \in [1.75, 2.25]$ and $\lambda \in [0.05, 0.075]$, in line with values reported by [27] and [13].

Despite pronounced topological differences across layers, the weighted in-degree distributions display remarkable regularity. By contrast, when restricting attention to tail-only fitting, confirming a truncated power law becomes substantially more difficult. In unreported results we reject H_0 for the long-term credit, cross-securities, and flattened layers, indicating alternative data-generating processes; however, these tail-only conclusions are weaker given the limited number of observations in the extreme tail.

The conclusions above depend on the network characteristic under study. In particular, when examining unweighted degree distributions (both in- and out-degree), we observe substantially more heterogeneity across layers, with evidence consistent with distinct data-generating processes. Researchers and practitioners should therefore be careful when simulating networks to represent specific segments of the interbank system and should ensure that the chosen representation reflects the underlying market relationships they aim to proxy.

¹⁷In this setting, higher confidence levels make it easier to confirm a truncated power-law data-generating process, whereas lower levels make confirmation more stringent.

Algorithm 1 Semi-parametric bootstrapped goodness-of-fit. We use default values of $B = X$.

Require: The number of bootstrapped samples $B > 0$, empirical data set x , candidate distribution

```

 $\mathbb{P}_{cand}(x)$ 
1:  $\hat{x}_{min}, KS_d, \hat{\alpha}, \hat{\lambda} \leftarrow \arg \min_{x_{min}} [\max_{x \geq x_{min}} |S(x) - \hat{P}(x)|]$ 
2:  $n \leftarrow |\{x\}|$ 
3:  $n_{tail} \leftarrow |\{x|x \geq x_{min}\}|$ 
4:  $n_{head} \leftarrow n - n_{tail}$ 
5:  $p \leftarrow 0$ 
6: for  $i = 1, \dots, B$  do
7:    $b \leftarrow \{\}$ 
8:   for  $j = 1, \dots, n$  do
9:     Sample random number  $\epsilon \sim U[0, 1]$ 
10:    if  $\epsilon < \frac{n_{tail}}{n}$  then
11:       $b.insert(x_i \sim \mathbb{P}_{cand}(x; \hat{x}_{min}, \hat{\alpha}, \hat{\lambda}))$ 
12:    else
13:       $b.insert(x_i \sim \mathbb{P}_{uniform}(\{x|x < x_{min}\}))$ 
14:    end if
15:  end for
16:   $KS_b \leftarrow \arg \min_{x_{min}} [\max_{x \geq x_{min}} |S(b) - \hat{P}(b)|]$ 
17:  if  $KS_d > KS_b$  then
18:     $p = p + 1$ 
19:  end if
20: end for
21:  $p = p/B$ 

```

1

Figure 3: The bootstrapping algorithm follows the semi-parametric procedure of [12] to assess the goodness-of-fit of heavy-tailed distributions. The approach can also be used when estimating a tail distribution with an estimated cut-off value \hat{x}_{min} .

Centrality measures

Centrality measures assess the centrality or degree of connection of a node within a specific layer of a multi-layer network. Typically, these metrics are derived from factors such as the number of connections, the significance of these connections, and the nodes they link, representing a node’s importance in the overall network structure [10]. While these measures may not be identical, they bear a resemblance to the concept of systemic importance extensively studied in finance and economics. Quantifying the primary drivers of systemic risk and attributing risk to individual contributors pose significant challenges [26]. Utilizing graph-based models for interbank markets and leveraging centrality measures present a promising approach to address some of these challenges. As emphasized by [18], theoretical literature on interbank networks offers a coherent method for studying interconnections, contagion processes, and systemic risk, albeit with certain limitations. Nevertheless, centrality measures can offer supplementary insights into the systemic significance of banks, surpassing traditional financial stability metrics.

In general, centrality measures yield the flexibility to introduce a ranking of nodes according to their

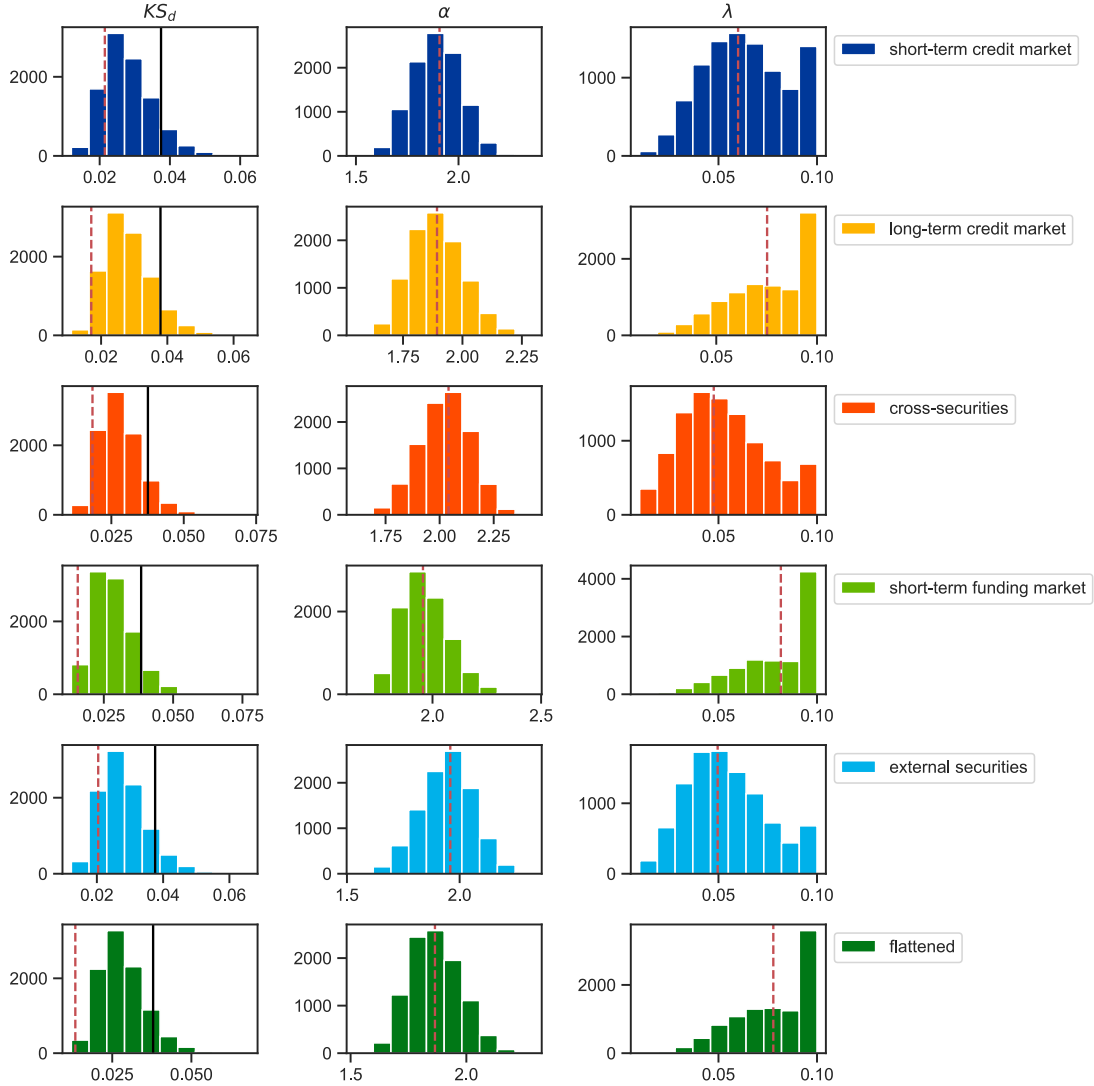


Figure 4: Semi-parametric bootstrapping results. Rows correspond to layers. The first column reports bootstrap Kolmogorov–Smirnov distances; the second column shows bootstrap lower-bound estimates \hat{x}_{\min} (when performing tail-only fits); the remaining columns report bootstrap parameter estimates (e.g., α and λ) for the truncated power law. The vertical red dashed line marks the non-bootstrapped estimate from the empirical data, and the solid black line indicates the 90th percentile of the bootstrap distribution.

tenor within a layer, allowing one to discover the most pivotal of nodes within the system [9]. Furthermore, a comparison of a centrality measure of the same node across different layers provides insights on the differences in the topology of layers. If a node is considered very central in one layer, but less central in another, then this underlines the different semantics of the layers.

We examine the cross-correlation patterns of various centrality measures across the layers. Figure 5 shows the Kendall Rank correlation matrices. The Kendall Rank correlation is a statistic used to measure the ordinal association between two measured quantities [19]. The Kendall correlation between two evaluators will be high (with an upper bound of 1) when observations have a similar ranking between the two evaluators and low (lower bound of -1) when observations have a dissimilar ranking between the evaluators. For our cause, we appoint the different layers as the evaluators, and analyze their agreement of which nodes are most central. The first observation from Figure 5 is that strictly positive correlations are observed for all centrality measures, hinting at some agreement between the layers. On a closer look, we see that most correlation values are between 30-60%, with an exception of the ranking correlation between the cross-securities market and the flattened network, which exceed the 80% mark for most centrality measures. Another exception is the Hubs measure for which low agreement is observed between most layers.

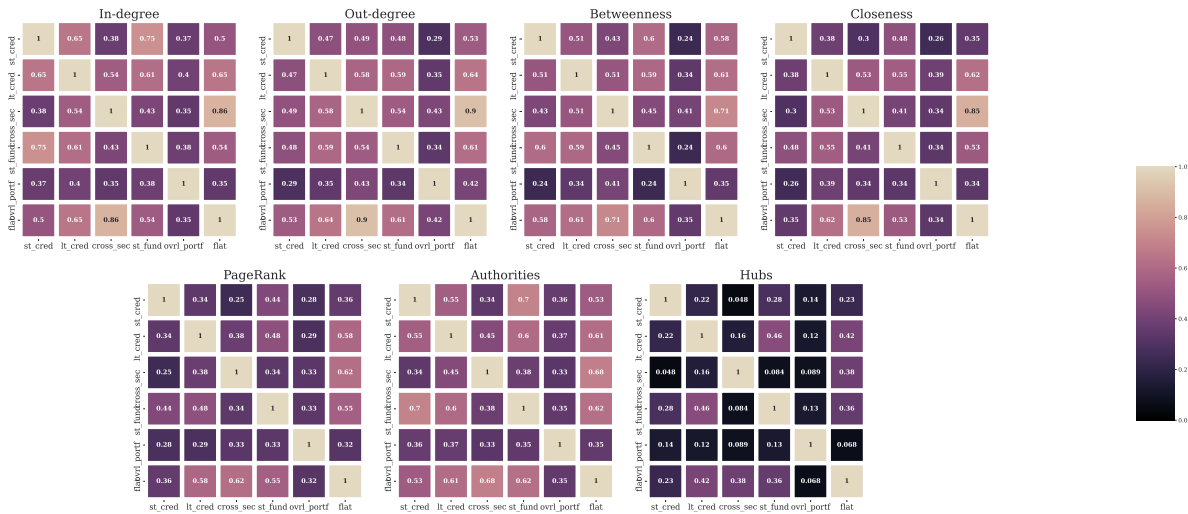


Figure 5: Each matrix represents the set of pairwise Kendall rank correlations based on a certain centrality measure. Names of the layers are abbreviated: short-term credit layer (st_cred), long-term credit layer (lt_cred), cross-securities layer (cross_sec), short-term funding layer (st_fund), overlapping portfolio layer (ovrl_portfl) and the flattened layer (flat). The figure has been created using [17].

To illustrate, we focus on node centrality assessed through the PageRank algorithm $C^{PR}(i)$. Figure 6 showcases the top 10 banking groups in various network layers, determined by their PageRank centrality scores. In each layer, the PageRank algorithm was applied, generating rankings to identify the most central banking groups within that specific layer. The results reveal clear heterogeneity between layers; certain nodes are highly central in one layer but not nearly as significant in another. For instance, the largest banking

group FR0 (depicted in green) ranks as the most central node in the short-term credit market but doesn't even make it to the top 10 central nodes in the cross-securities market. Similar disparities are observed for other nodes in the network.

In accordance with the Kendall Rank correlation matrices, we find a level of centrality persistence across layers, indicating that nodes ranked highly within one layer are more likely to be within the top 20% percentile in other layers. However, this persistence is not precise; within this top 20%, there is considerable heterogeneity, with nodes that are top-ranked in one layer not necessarily maintaining top positions in other layers.

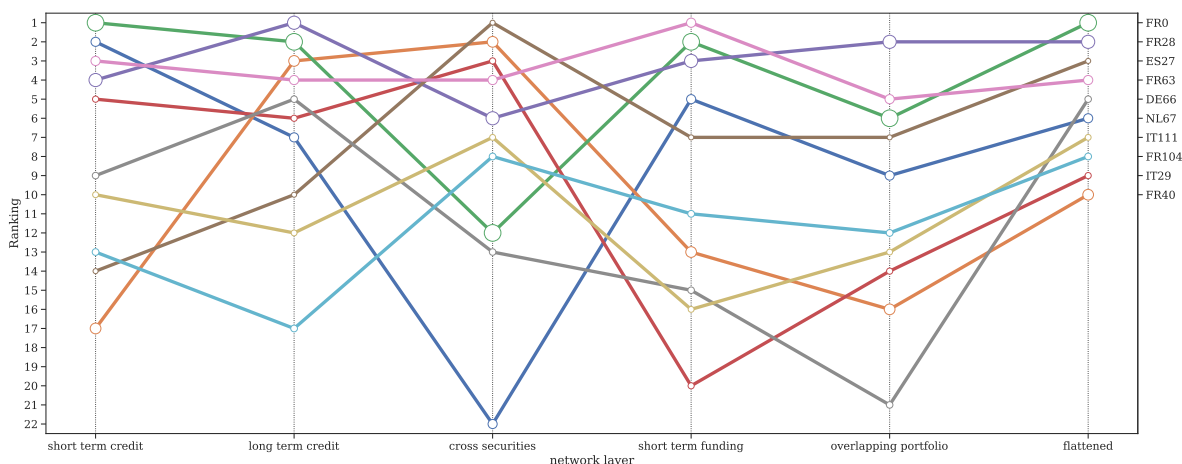


Figure 6: The ranking of the 10 largest banking groups by the PageRank algorithm $C^{PR}(i)$ across different layers of the multi-layer network. Banking groups are color-coded and the size of the markers is proportional to the total assets of the banking groups. The figure has been created using [17].

Concluding remarks

In this paper, we demonstrate that recent Euro Area granular data collections serve as a robust foundation for constructing and analyzing multi-layer networks. The multi-layer network framework described in our work provides a natural and effective means to represent granular data, enabling a comprehensive understanding of the topological structure of the EA financial interbank system. Our analysis sheds light on the intricate nature of contemporary interbank markets, offering insights into a wide spectrum of network layers and their diverse topological properties. By benchmarking the real-world data-derived network against common theoretical assumptions, our findings underscore the necessity for researchers and practitioners to exercise caution when simulating networks to target specific segments of the interbank network. It is important to acknowledge and incorporate the intricacies inherent in the financial markets being modeled. That is, some assumptions (e.g., small-world properties or power-law behaviour) are valid for only a certain type of financial relationship between banking groups.

Bibliography

- [1] Daan in 't Veld and Iman van Lelyveld. "Finding the core: Network structure in interbank markets". In: *Journal of Banking and Finance* 49 (2014), pp. 27–40.
- [2] Iñaki Aldasoro and Ivan Alves. "Multiplex interbank networks and systemic importance: An application to European data". In: *Journal of Financial Stability* 35 (2018), pp. 17–37.
- [3] Franklin Allen and Ana Babus. "Networks in finance". In: *The network challenge: strategy, profit, and risk in an interlinked world*. Wharton School Publishing, 2009, p. 367.
- [4] Jeff Alstott, Ed Bullmore, and Dietmar Plenz. "powerlaw: A Python Package for Analysis of Heavy-Tailed Distributions". In: *PLoS ONE* 9.1 (Jan. 2014). Ed. by Fabio Rapallo, e85777. DOI: [10.1371/journal.pone.0085777](https://doi.org/10.1371/journal.pone.0085777). URL: <https://doi.org/10.1371%2Fjournal.pone.0085777>.
- [5] Olivier De Bandt, Philipp Hartmann, and José Luis Peydró. *Systemic Risk in Banking*. Oxford University Press, 2012.
- [6] Leonardo Bargigli et al. "The multiplex structure of interbank networks". In: *Quantitative Finance* 15.4 (2015), pp. 673–691.
- [7] Federico Battiston, Vincenzo Nicosia, and Vito Latora. "Structural measures for multiplex networks". In: *Physical Review E* 89.3 (2014), p. 032804.
- [8] Stefano Battiston et al. "DebtRank: Too central to fail? financial networks, the FED and systemic risk". In: *Scientific reports* 2.1 (2012), pp. 1–6.
- [9] Francis Bloch, Matthew O Jackson, and Pietro Tebaldi. "Centrality measures in networks". In: *Social Choice and Welfare* 61 (2023), pp. 413–453. DOI: [10.1007/s00355-023-01456-4](https://doi.org/10.1007/s00355-023-01456-4).
- [10] Stephen P. Borgatti and Martin G. Everett. "A Graph-theoretic perspective on centrality". In: *Social Networks* 28.4 (Oct. 2006), pp. 466–484. DOI: [10.1016/j.socnet.2005.11.005](https://doi.org/10.1016/j.socnet.2005.11.005). URL: <https://doi.org/10.1016/j.socnet.2005.11.005>.
- [11] Michael Boss et al. "Network topology of the interbank market". In: *Quantitative finance* 4.6 (2004), pp. 677–684.
- [12] Aaron Clauset, Cosma Rohilla Shalizi, and M. E. J. Newman. "Power-Law Distributions in Empirical Data". In: *SIAM Review* 51.4 (Nov. 2009), pp. 661–703. DOI: [10.1137/070710111](https://doi.org/10.1137/070710111). URL: <https://doi.org/10.1137/070710111>.
- [13] Rama Cont, Amal Moussa, and Edson B Santos. *Network structure and systemic risk in banking systems*. Post-Print. HAL, 2013. URL: <https://EconPapers.repec.org/RePEc:hal:journl:hal-00912018>.
- [14] Antonio Di Cesare and Anna Rogantini Picco. *A survey of systemic risk indicators*. Occasional Paper 458. Bank of Italy, 2018. URL: <https://ssrn.com/abstract=3398812>.
- [15] Janina Engel, Michela Nardo, and Michela Rancan. "Network Analysis for Economics and Finance: An Application to Firm Ownership". In: *Data Science for Economics and Finance: Methodologies and Applications*. Ed. by Sergio Consoli, Diego Reforgiato Recupero, and Michaela Saisana. Cham: Springer International Publishing, 2021, pp. 331–355. ISBN: 978-3-030-66891-4. DOI: [10.1007/978-3-030-66891-4_14](https://doi.org/10.1007/978-3-030-66891-4_14). URL: https://doi.org/10.1007/978-3-030-66891-4_14.
- [16] Juan Carlos González-Avella, Vanessa Hoffmann de Quadros, and José Roberto Iglesias. "Network topology and interbank credit risk". In: *Chaos, Solitons and Fractals* 88 (July 2016), pp. 235–243. DOI: [10.1016/j.chaos.2015.11.044](https://doi.org/10.1016/j.chaos.2015.11.044). URL: <https://doi.org/10.1016/j.chaos.2015.11.044>.
- [17] J. D. Hunter. "Matplotlib: A 2D graphics environment". In: *Computing in Science & Engineering* 9.3 (2007), pp. 90–95. DOI: [10.1109/MCSE.2007.55](https://doi.org/10.1109/MCSE.2007.55).
- [18] Anne-Caroline Hüser. *Too interconnected to fail: A survey of the Interbank Networks literature*. SAFE Working Paper Series 91. Leibniz Institute for Financial Research SAFE, 2016.

- [19] M. G. Kendall. *Rank Correlation Methods*. London: Griffin, 1970.
- [20] L. Markovich. “Light- and Heavy-Tailed Density Estimation by Gamma-Weibull Kernel”. In: *Springer Proceedings in Mathematics and Statistics*. Springer International Publishing, 2018, pp. 145–158. doi: [10.1007/978-3-319-96941-1_10](https://doi.org/10.1007/978-3-319-96941-1_10). URL: https://doi.org/10.1007/978-3-319-96941-1_10.
- [21] Staša Milojević. “Power law distributions in information science: Making the case for logarithmic binning”. In: *Journal of the American Society for Information Science and Technology* 61.12 (Dec. 2010), pp. 2417–2425. doi: [10.1002/asi.21426](https://doi.org/10.1002/asi.21426). URL: <https://doi.org/10.1002/asi.21426>.
- [22] Mattia Montagna and Christoffer Kok. *Multi-layered interbank model for assessing systemic risk*. Working Paper Series. European Central Bank, 2016.
- [23] Mattia Montagna and Thomas Lux. “Contagion risk in the interbank market: a probabilistic approach to cope with incomplete structural information”. In: *Quantitative Finance* 17.1 (May 2016), pp. 101–120. doi: [10.1080/14697688.2016.1178855](https://doi.org/10.1080/14697688.2016.1178855). URL: <https://doi.org/10.1080/14697688.2016.1178855>.
- [24] Kimmo Soramäki and Samantha Cook. “SinkRank: An Algorithm for Identifying Systemically Important Banks in Payment Systems”. In: *Economics* 7.1 (June 2013). doi: [10.5018/economics-ejournal.ja.2013-28](https://doi.org/10.5018/economics-ejournal.ja.2013-28). URL: <https://doi.org/10.5018/economics-ejournal.ja.2013-28>.
- [25] Kimmo Soramäki et al. “The topology of interbank payment flows”. In: *Physica A: Statistical Mechanics and its Applications* 379.1 (2007), pp. 317–333. URL: <https://EconPapers.repec.org/RePEc:eee:phsmap:v:379:y:2007:i:1:p:317-333>.
- [26] Nikola Tarashev, Claudio Borio, and Kostas Tsatsaronis. “The systemic importance of financial institutions”. In: *BIS Quarterly Review* (Sept. 2009). URL: <https://ideas.repec.org/a/bis/bisqtr/0909h.html>.
- [27] Benjamin Vandermarliere et al. “Beyond the power law: Uncovering stylized facts in interbank networks”. In: *Physica A: Statistical Mechanics and its Applications* 428 (June 2015), pp. 443–457. doi: [10.1016/j.physa.2015.01.058](https://doi.org/10.1016/j.physa.2015.01.058). URL: <https://doi.org/10.1016/j.physa.2015.01.058>.
- [28] Pauli Virtanen et al. “SciPy 1.0: Fundamental Algorithms for Scientific Computing in Python”. In: *Nature Methods* 17 (2020), pp. 261–272. doi: [10.1038/s41592-019-0686-2](https://doi.org/10.1038/s41592-019-0686-2).
- [29] Quang H. Vuong. “Likelihood Ratio Tests for Model Selection and Non-Nested Hypotheses”. In: *Econometrica* 57.2 (Mar. 1989), p. 307. doi: [10.2307/1912557](https://doi.org/10.2307/1912557). URL: <https://doi.org/10.2307/1912557>.
- [30] Duncan J. Watts and Steven H. Strogatz. “Collective dynamics of ‘small-world’ networks”. In: *Nature* 393.6684 (June 1998), pp. 440–442. doi: [10.1038/30918](https://doi.org/10.1038/30918). URL: <https://doi.org/10.1038/30918>.